Fractal dimension fluctuations for snapshot attractors of random maps

Arthur Namenson
Naval Research Laboratory, Washington, D.C. 20375

Edward Ott* and Thomas M. Antonsen
Department of Electrical Engineering, Department of Physics, and Institute for Plasma Research, University of Maryland, College Park, Maryland 20742

(Received 18 September 1995)

We consider the determination of the information dimension of a fractal snapshot attractor (i.e., the pattern formed by a cloud of orbits at a fixed time) of a random map. It is found that box-counting estimates of the dimension fluctuate from realization to realization of the random process. These fluctuations about the true dimension value are a result of the unavoidable presence of a finite smallest box size ϵ_* used in the dimension estimation. The main result is that the fluctuations are well described by a Gaussian probability distribution function whose width is proportional to $(\log 1/\epsilon_*)^{-1/2}$. Averaging dimension estimates over many realizations (or over time for a single realization) thus yields a means of obtaining a greatly improved estimate of the true dimension value.

PACS number(s): 05.45.+b, 02.50.−r

I. INTRODUCTION

In this paper we consider random maps

$$\mathbf{x}_{n+1} = \mathbf{M}_n(\mathbf{x}_n), \tag{1}$$

where, on each iterate n, the map function $\mathbf{M}_n$ is chosen randomly from an ensemble of map functions according to some probability distribution function. For simplicity, we will henceforth specialize to the case where $\mathbf{M}_n$ is a given function (fixed in time n) of a random scalar parameter c_n,

$$\mathbf{M}_n(\mathbf{x}) = \mathbf{M}(\mathbf{x}, c_n),$$

where c_n is chosen randomly on each iterate with a probability distribution function that we denote $P(c)$.

The dynamics generated by random maps has recently been the subject of theoretical study [1]. In addition, random maps are of interest as models of advection by temporally irregular fluid flows [2–6]. Indeed, in recent experimental papers [3] the authors made explicit use of random maps to discuss and analyze their results. These experiments dealt with the fractal patterns formed by a scum of floating particles on the surface of a fluid that was undergoing temporally irregular motion. The motion of the floating particles was chaotic in the sense that the positions of nearby particles diverged exponentially from each other with time. Furthermore, as explained later in Sec. II, the particle motion was on average compressive, so that the describing two-dimensional map is area shrinking (dissipative) rather than area preserving (conservative).

Under such circumstances one expects the particles to be attracted to a fractal pattern, similar to the strange attractor of a chaotic nonrandom map. One difference here is that, because of the random time dependence of the map, the pattern is not steady with time but moves around in a random way. Thus we speak of a "snapshot attractor," which is a picture of the fractal pattern at a given instant in time [1–5,7]. More precisely, say we initiate a smooth density of orbit points at some negative time $-n_0$. We then map this density forward in time using the random map and examine the density at some positive time n. Now imagine that we keep n fixed and increase n_0. To increase n_0 by one, we keep all the same $\mathbf{M}_n$ of the random realization, but add one new randomly chosen $\mathbf{M}_n$ at the *beginning* of the sequence. As n_0 increases, the pattern at time n becomes more and more fine scaled, approaching a spatially fixed fractal attractor in the limit as $n_0 \to \infty$ [1–5,7].

While the pattern generated in the above manner is substantially different if n is changed, the dimension of the pattern is the same for all n. Indeed Ladrappier and Young [1] prove that, with probability one, a given realization of the random process will result in a sequence of patterns each having an information dimension given by the Kaplan-Yorke formula [8], which for the two-dimensional cases of interest to us here is

$$D_{\mathrm{KY}} = 1 + (h_1/|h_2|). \tag{2}$$

Here h_1 and h_2 are the Lyapunov exponents, one of which, h_1, is positive (chaos), while the other, h_2, is negative and satisfies $h_1 + h_2 < 0$ (area contraction).

In practice the information dimension of a fractal attractor is most commonly obtained by box counting

*Also at Institute for Systems Research, University of Maryland, College Park, MD 20742.

(e.g., this is the method employed in the experiments in Ref. [3]). To define the information dimension by box counting, imagine that we divide the area into a grid of boxes of size ϵ and then calculate the fraction of particles (measure) of the snapshot attractor in each box. The information dimension is then defined by

$$D_I = \lim_{\epsilon \to 0} I(\epsilon)/\log(1/\epsilon), \tag{3}$$

where the information $I(\epsilon)$ is given by

$$I(\epsilon) = -\sum_i \mu_i \log \mu_i \tag{4}$$

and μ_i is the measure in box i. In real situations, however, the limit of ϵ going to zero cannot be taken. Instead, one estimates D_I by first calculating $I(\epsilon)$ for a range of ϵ values down to some minimum ϵ_* and then fitting a straight line to the data for $I(\epsilon)$ versus $\log(1/\epsilon)$ in the available ϵ range. The estimated D_I (which we denote $D_{\rm BC}$) is then taken as the slope of the fitted line.

The main points of this paper are as follows: (i) for small but nonzero ϵ_*, such dimension estimates fluctuate from realization to realization of the random process, (ii) the fluctuations conform to a Gaussian distribution, and (iii) the width of the Gaussian scales as $(\log 1/\epsilon_*)^{-1/2}$. Thus, as $\epsilon_* \to 0$, the width of the distribution goes to zero and almost every realization gives the same value [Eq. (2)], as it should.

The above implies that averaging of dimension estimates over many random realizations yields a means of obtaining an improved estimate of the true dimension value (i.e., the box-counting value that would apply to every realization if $\epsilon_* \to 0$). Alternatively, the stationarity of the random process implies that the average over realizations can be replaced by averaging over different snapshots taken at different times for a single realization (this was done in the experiments in Ref. [3]).

In Sec. II we introduce an illustrative random map previously used [2] to model the evolution of the pattern of scum floating on a fluid surface. This map is then used in numerical experiments and the information dimension of the resulting snapshot attractor is estimated using the previously described box-counting method. This is repeated for many realizations of the random map process and the estimated dimension values are shown to be well described by a Gaussian distribution about the true value, which we obtain to high accuracy using (2).

Section III considers a random baker's map model for which explicit results are easily obtained. It is shown analytically for this model that the fluctuation in dimension estimates is Gaussian and that the width of the distribution scales as $(\log 1/\epsilon_*)^{-1/2}$. Based on the results of Secs. II and III, we conjecture that results (i)–(iii) above apply very generally.

II. NUMERICAL EXPERIMENTS ON A MODEL RANDOM MAP

A. Model

We now consider a model random map [2,4] given by

$$x_{n+1} = [x_n + y_n(1 - e^{-\alpha})/\alpha] \bmod 2\pi, \tag{5a}$$

$$y_{n+1} = \kappa \sin(x_{n+1} + c_n) + e^{-\alpha} y_n, \tag{5b}$$

where c_n is chosen randomly in $[0, 2\pi]$ at each iterate (i.e., the probability distribution of c is $P(c) = (2\pi)^{-1}$ in $[0, 2\pi]$). In what follows we take $\alpha = 0.09$ and $\kappa = 0.5$. The Jacobian determinant of the map (5) is $e^{-\alpha}$ independent of x and y. Thus areas are contracted by the factor $e^{-\alpha} < 1$ on each iterate and $h_1 + h_2 = -\alpha$, which when used in (2) yields

$$D_{\rm KY} = 1 + h_1/(h_1 + \alpha). \tag{6}$$

In the case with no randomness and c_n set to zero (5) reduces to the map introduced by Zaslavsky in Ref. [10].

As a physical motivation for (5) consider floating particles on the surface ($z = 0$) of a fluid located in the region $z < 0$. Assume [2] that the fluid flow consists of three incompressible components $\mathbf{v} = \mathbf{v}_1 + \mathbf{v}_2 + \mathbf{v}_3$, where $\mathbf{v}_1$ is a steady horizontal shear flow given by $\mathbf{v}_1 = v_0 y \mathbf{x}_0$, $\mathbf{v}_2$ is a steady down welling given by $\mathbf{v}_2 = -u_0 y \mathbf{y}_0 + u_0 z \mathbf{z}_0$, and $\mathbf{v}_3$ is a temporally irregular vortical component modeled as

$$\mathbf{v}_3(x, y, t) = \omega_0 \sin[x + c(t)] \sum_m \delta(t - mT) \mathbf{y}_0.$$

Here $c(t)$ is a temporally irregular function of time and $c_n \equiv c(nT)$ is modeled as a random variable. Setting $z = 0$ (appropriate for floating particles) and integrating the particle position from just after the nth δ-function pulse to just after the $(n+1)$th δ-function pulse, we obtain (5) after suitable rescaling. Note that the divergences of $\mathbf{v}_1$, $\mathbf{v}_2$, and $\mathbf{v}_3$ in the full three-dimensional space are each zero, but that the divergence restricted to the surface $z = 0$ is negative, $\nabla' \cdot \mathbf{v} \equiv [\partial v_x/\partial x + \partial v_y/\partial_y]_{z=0} = \nabla' \cdot \mathbf{v}_2 = -u_0$, thus leading to area contraction by the map.

B. Numerical experiments on the map given by Eqs. (5)

Snapshot attractors were generated by first randomly sprinkling 10^6 initial conditions uniformly in the region $0 \le x \le 2\pi$, $-2 \le y \le 2$. These initial conditions were then each iterated using the same randomly chosen sequence of phase angles $\{c_n\}$. After a large number of iterates, the positions of all the orbits were recorded and these positions were regarded to represent the snapshot. Using 40 different random realizations of the sequence $\{c_n\}$, 40 different snapshots were generated. Figure 1 shows a representative snapshot attractor generated in the above manner.

For each snapshot we performed a box-counting determination of the information dimension, by first dividing the region $0 \le x \le 2\pi$, $-2 \le y \le 2$ into 2^{2p} boxes of dimension $\Delta x = 2\pi\epsilon$ by $\Delta y = 4\epsilon$ where $\epsilon = 2^{-p}$. We then estimated the measure μ_i of each of the 2^{2p} boxes as the fraction of the 10^6 orbit points in that box and we

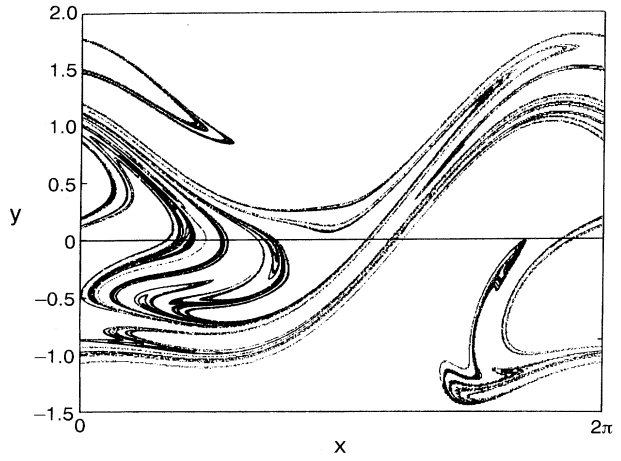

FIG. 1. Snapshot attractor of Eqs. (5).

did this for successively smaller values of ϵ (larger values of p). The slope of the best-fit straight line to the numerical data for $I(\epsilon)$ versus $\log(1/\epsilon)$ was taken for ϵ in the range $2^{-1} \geq \epsilon \geq \epsilon_* = 2^{-10}$ for each of the 40 realizations and constitute our estimates of the information dimension. The cutoff at $\epsilon_* = 2^{-10}$ was chosen because, for smaller ϵ, it was found that the estimates of the measures μ_i are degraded by the effect of the finite number of orbits (namely, 10^6).

The 40 box-counting estimates of the information dimension were found to have small fluctuations about a mean value. As explained below, these fluctuations are consistent with a Gaussian distribution whose mean and standard deviation are

$$\bar{D}_{\mathrm{BC}} = 1.51 \pm 0.01, \tag{7a}$$

$$\sigma = 0.05 \pm 0.01. \tag{7b}$$

To test consistency with a Gaussian distribution we utilize the "probability plot" technique [11]. This is a method for determining if the sample of N measurements $(z_1, z_2, \ldots, z_N)$ is consistent with these measurements being drawn from a probability distribution $\phi(z)$. In our case the measurements z_i are the 40 box-counting dimension estimates and $\phi(z)$ is taken to be a Gaussian distribution function. The method is to first reorder the measurements so that they are ranked by size (that is, $z_i \leq z_{i+1}$ for $0 < i \leq N$). Then the mean cumulative frequency $p_i = i/N$ is plotted against z_i. However, p_i is plotted on a nonlinear scale as follows: if $F(z) = \int_{-\infty}^{z} \phi(z')dz'$ is the cumulative distribution function, then the distance from the origin along the vertical (p_i) axis is proportional to $F^{-1}(p_i)$. Thus, if the measurements are indeed drawn from a Gaussian distribution, then the resulting plot will approximate a straight line. As shown in Fig. 2, this is the case.

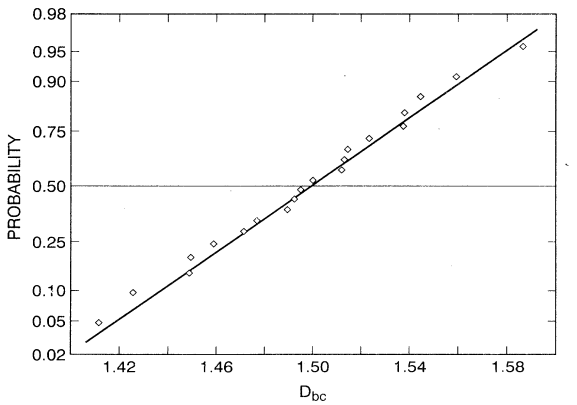

FIG. 2. Probability plot.

We also determined an accurate value of the positive Lyapunov exponent h_1 by iterating the Jacobian matrix of (5) for 10^7 iterates. Several repetitions with different random realizations yielded the same value of h_1 to within three decimal places, namely, $h_1 = 0.987$. Inserting this value in Eq. (6), we obtain $D_{\mathrm{KY}} = 1.52$, in agreement with the value of $\bar{D}_{\mathrm{BC}}$ in (7a).

III. RANDOM BAKER'S MAP

In this section we consider a simple solvable random map model for which the dimension fluctuation properties can be explicitly demonstrated analytically. The map is

$$x_{n+1} = \begin{cases} \lambda x_n & \text{if } y_n \leq c_n \\ \frac{1}{2} + \lambda x_n & \text{if } y_n > c_n, \end{cases} \tag{8a}$$

$$y_{n+1} = \begin{cases} y_n/c_n & \text{if } y_n \leq c_n \\ (y_n - c_n)/d_n & \text{if } y_n > c_n, \end{cases} \tag{8b}$$

where $0 < \lambda < 1/2$, $d_n \equiv 1 - c_n$, and c_n is restricted to lie in $(0, 1)$ and is chosen randomly on each iterate. The variables (x, y) are considered to lie in the unit square $0 \leq (x, y) \leq 1$. The action of the map is illustrated schematically in Fig. 3.

Using the same notation as in the preceding section, we assume that a smooth particle density is initialized at time $-n_0$ where $n_0 > 0$. As a result of the uniform stretching of (8b), the particle distribution at fixed n be-

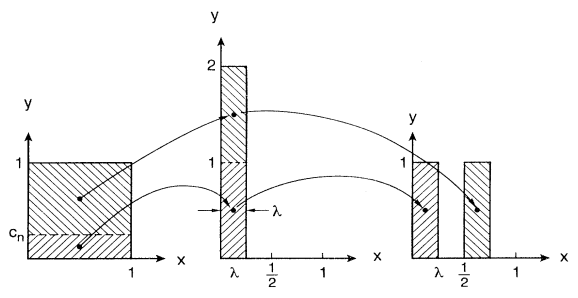

FIG. 3. Schematic illustration of the action of the random baker's map Eqs. (8) on the unit square.

comes uniform in $0 \leq y \leq 1$ as $n_0 \to +\infty$. We now consider the determination of D_{BC} for the measure projected onto the x axis using a minimum interval size $\epsilon_* = \lambda^m$. Without loss of generality, we can fix the time at $n = 0$. With this model the information $I(\epsilon)$ for $\epsilon = \lambda^k (k = 0, 1, \ldots, m)$ is

$$I(\lambda^k) = \sum_{j=1}^{k} \Delta_j, \tag{9a}$$

where

$$\Delta_j = -(c_{-j} \log c_{-j} + d_{-j} \log d_{-j}). \tag{9b}$$

To obtain (9) first consider $k = 1$. We note that the measure is uniform in y at all finite times (we have taken the limit $n_0 \to +\infty$) and that the measure at time $n = 0$ results from one iteration of the measure at time $n = -1$. Thus the measure at $n = 0$ lies in the two λ-width strips in Fig. 3, with the left strip having a measure c_{-1} and the right strip having a measure d_{-1}. Hence we have (9) for $k = 1$. To establish (9) for $k > 1$ one can now proceed by induction. We omit the details.

Equations (9) can be rewritten by separating Δ_j into an average and a fluctuation $\Delta_j = \langle \Delta \rangle + \delta_j$,

$$I(\lambda^k) = k\langle \Delta \rangle + \sum_{j=1}^{k} \delta_j, \tag{10}$$

where $\langle \Delta \rangle$ is the average of $-(c \log c + d \log d)$ over the probability distribution of c. Since the c's are chosen randomly on each iterate the δ_j are zero mean, independent, identically distributed random variables. Thus (9a) represents a Brownian random walk (biased by $\langle \Delta \rangle$) of length k and a graph of $I(\lambda^k)$ versus $\log(1/\epsilon) = k \log(1/\lambda)$ is essentially the graph of the position of a biased Brownian random walker versus time. As k increases the root mean squared fluctuation in (10), $\langle (\sum \delta_j)^2 \rangle^{1/2}$, increases like $k^{1/2}$. Thus, for $k \to \infty$ the term $k\langle \Delta \rangle$ dominates and, with probability one, we obtain the same dimension for all realizations,

$$D_I = \langle \Delta \rangle / \log(1/\lambda), \tag{11}$$

which also agrees with (2). Thus, to establish the result that, for small ϵ_*, D_{BC} has a Gaussian distribution with width scaling like $(\log 1/\epsilon_*)^{-1/2}$, we need only show that the slope of the least-squares best-fit straight line to $\sum_{j=1}^{k} \delta_j$ versus k for $0 \leq k \leq k_*$ has a Gaussian distribution with width proportional to $k_*^{-1/2}$. This is done in the Appendix.

IV. CONCLUSION

In conclusion, we have shown that box-counting dimension estimates of random map fractal attractors fluctuate about a mean value from realization to realization and these fluctuations are Gaussian with a width that scales like $(\log 1/\epsilon_*)^{-1/2}$, where ϵ_* is the smallest box size in the dimension estimate.

ACKNOWLEDGEMENT

This work was supported in part by the Office of Naval Research.

APPENDIX

We consider the function

$$f(k) = \sum_{j=1}^{k} \delta_j, \tag{A1}$$

where $f(0) = 0$ and δ_k are zero mean, independent, identically distributed random variables. For a given realization $\{\delta_j\}$, let $ak + b$ denote the least-squares best-fit straight line to $f(k)$ in the range $0 \leq k \leq k_*$. We want to show that a has a Gaussian distribution with width proportional to $k_*^{-1/2}$. Minimizing the mean squared error

$$E = \sum_{k=0}^{k_*} [f(k) - (ak + b)]^2 \tag{A2}$$

with respect to a and b, we obtain

$$a \cong \frac{6}{k_*} \left\{ \frac{\sum k f(k)}{\sum k} - \frac{\sum f(k)}{k_*} \right\} \tag{A3}$$

for $k_* \gg 1$. Substituting (A1) in (A3) and expanding for $k_* \gg 1$ we obtain after some algebra

$$a \cong -\frac{3}{k_*^3} \sum_{j=1}^{k_*-1} j^2 \delta_{k_*-j}. \tag{A4}$$

Thus $\langle a^2 \rangle \cong (9/k_*^6)\langle \delta^2 \rangle \sum j^4 \cong (9/5)\langle \delta^2 \rangle / k_*$ and hence $\langle a^2 \rangle^{1/2} \sim k_*^{-1/2}$, as previously claimed. We now show that (15) yields a Gaussian distribution. Let $p(\delta)$ and $q(\bar{a})$ be the probability distributions of δ and $\bar{a} \equiv -k_*^3 a/3$. Let $\tilde{p}(\kappa)$ and $\tilde{q}(\kappa)$ be the Fourier transforms of $p(\delta)$ and $q(\bar{a})$ with transform variable κ. Equation (A4) yields

$$\tilde{q}(\kappa) = \tilde{p}(\kappa)\tilde{p}(2^2\kappa) \cdots \tilde{p}((k_* - 1)^2 \kappa). \tag{A5}$$

Noting that $\tilde{p}(\kappa)$ is maximum at $\kappa = 0$ and that, by virtue of the Fourier transform $\partial^2 \tilde{p}/\partial \kappa^2|_{\kappa=0} = -\langle \delta^2 \rangle$, we have

$$\tilde{p}(\kappa) \cong 1 - \frac{1}{2}\langle \delta^2 \rangle \kappa^2 \cong \exp\left(-\frac{1}{2}\langle \delta^2 \rangle \kappa \right) \tag{A6}$$

for small κ. Putting (A6) in (A5) we obtain for $\tilde{q}(\kappa)$ a Gaussian in κ,

$$\tilde{q}(\kappa) \cong \exp\left(-\left\{ \frac{\langle \delta^2 \rangle}{10} k_*^5 \kappa^2 \right\} \right). \tag{A7}$$

The inverse Fourier transform of (A7) is thus a Gaussian in $\bar{a}$ for $q(\bar{a})$.

[1] F. Ladrappier and L.-S. Young, Commun. Math. Phys. **117**, 529 (1988).
[2] L. Yu, E. Ott, and Q. Chen, Phys. Rev. Lett. **65**, 2935 (1990); Physica D **53**, 102 (1991).
[3] J. C. Sommerer and E. Ott, Science **259**, 335 (1993); J. C. Sommerer, Physica D **76**, 85 (1994).
[4] A. Namenson, T. M. Antonsen, and E. Ott (unpublished).
[5] J. C. Sommerer (unpublished).
[6] Area preserving random maps modeling passive scalar transport through the volume of a fluid have been considered in the following references. F. Varosi *et al.*, Phys. Fluids A **3**, 1017 (1991); E. Ott and T. M. Antonsen, Phys. Rev. Lett. **61**, 2839 (1988); T. M. Antonsen and E. Ott, Phys. Rev. A **44**, 851 (1991).
[7] F. J. Romeiras, C. Grebogi, and E. Ott, Phys. Rev. A **41**, 784 (1990).
[8] J. Kaplan and J. A. Yorke, in *Functional Differential Equations and Approximations of Fixed Points*, edited by H.-O. Peitgen and H.-O. Walter, Springer Lecture Notes in Mathematics, Vol. 730 (Springer, Berlin, 1978), p. 228; see also Sec. 4.4 of Ref. [9] and references therein.
[9] E. Ott, *Chaos in Dynamical Systems* (Cambridge University Press, Cambridge, 1993).
[10] G. M. Zaslavsky, Phys. Lett. **69A**, 145 (1978).
[11] J. M. Juran, F. M. Gryna, Jr., and R. S. Bingham, *Quality Control Handbook* (McGraw-Hill, New York, 1974), pp. 2210–2213.